

Development of a guiding system and visual feedback real-time controller for the high-speed self-align optical cable winding[†]

Changwoo Lee¹, Hyunkyoo Kang², and Keehyun Shin^{2,*}

¹*Flexible Display Roll to Roll Research Center, Konkuk University, Seoul, 143-701, Korea*

²*Department of Mechanical Engineering, Konkuk University, Seoul, 143-701, Korea*

(Manuscript Received January 7, 2007; Revised July 8, 2008; Accepted August 7, 2007)

Abstract

Recently, the demand for the optical cable has been rapidly growing because of the increasing number of internet users and the high speed internet data transmission required. But the present optical cable winding systems have some serious problems such as pile-up and collapse of cables usually near the flange of the bobbin in the process of cables winding. To reduce the pile-up collapse in cable winding systems, a new guiding system is developed for a high-speed self-align cable winding. First, mathematical models for the winding process and bobbin shape fault compensation were proposed, the winding mechanism was analyzed and synchronization logics for the motions of winding, traversing, and the guiding were created. A prototype cable winding systems was manufactured to validate the new guiding system and the suggested logic. Experiment results showed that the winding system with the developed guiding system outperformed the system without the guiding system in reducing pile-up and collapse in high-speed winding.

Keywords: Guiding system; Optical cable; Pile up and collapse; Real-time scheduling; Traversing; Task; Visual feedback control

1. Introduction

The relatively large-diameter and rigid cables such as optical cables or power lines may not wind closely near the flange of a bobbin and thus leave some gap in the process of winding around the circular bobbin. In addition, during the winding process, due to the problems such as defects in the shape of the bobbin, change of cable diameter, traversing and velocity synchronization of the bobbin, and tension control, the pile-up and collapse phenomenon of the cable frequently occur, thereby becoming major causes of increasing the percentage of defective products and decreasing productivity. To solve these problems, a cable aligning process is carried out manually. However, method is completely not suit-

able for maintaining high quality productivity.

With the growth of communication technology as well as internet-based industry, the demand for an optical data cable increases rapidly. Therefore, a high speed self align guiding system needs to be developed. Previous studies [1, 2] on the winding logic at the condition that can easily bend a material itself, as in fiber or general electric wire in which rigidity is not high, have been reported, but any guiding system for the high-speed self-align winding of the materials that do not easily bend with very high rigidity, such as an optical cable, has not been reported yet. In this study, a high-speed self-align cable guiding system has been developed. To develop the guiding system, we analyzed the problems in the field systematically, interpreted the characteristics of the winding system by developing mathematical models on the winding process of cables with various diameters and bobbin shape error, and developed a real-time controller that can minimize winding faults caused by a defect in the shape of the bobbin and diameter

[†] This paper was recommended for publication in revised form by Associate Editor Dae-Eun Kim

*Corresponding author. Tel.: +82 2 450 3072, Fax.: +82 2 447 5886

E-mail address: khshin@konkuk.ac.kr

© KSME & Springer 2008

change of material, through visual feedback and real-time motion synchronization.

By a simulator manufactured in a 1/10 size of the actual one, the characteristics of the guiding system were verified at high speeds.

2. Mathematical models for high speed cable winding system

2.1 An ideal winding process model

Fig. 1 illustrates an ideal case of a cable stack up around the bobbin; U indicates the linear velocity of the process, and V , the traversing velocity of the bobbin.

In the winding process, because the winding diameter increases by the cable diameter as the cable stacks up on a new layer, the linear velocity becomes higher than a reference value. This change of velocity generates tension disturbance deteriorating the winding state of the cable [3].

The revolving angular velocity (w) of the bobbin in Fig. 1 is the same as Eq. (1), and the time (t) it takes for the bobbin to revolve around can be found from Eq. (2). Where, H is the winding diameter. As the cable traverses as much as its diameter while the bobbin revolves around, the traversing velocity is derived as the following Eq. (3) from Eqs. (1)-(2).

Fig. 2 shows the respective winding diameter in respect of each layer when the cable is wound, and in case of winding the first layer, the summation of the bobbin diameter (D) and cable diameter (d) is defined as Eq. (4). The winding diameter when winding

$$w = \frac{2U}{H} \tag{1}$$

$$t = \frac{2\pi}{w} \tag{2}$$

$$V = \frac{d}{t} = \frac{dw}{2\pi} \tag{3}$$

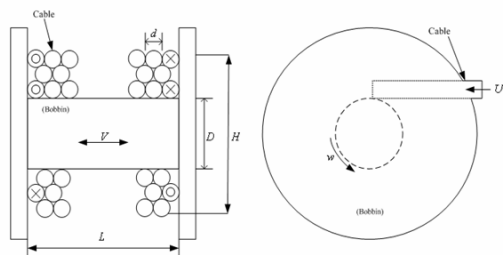


Fig. 1. Schematic of cable winding.

the second layer in Fig. 2 is expressed as Eq. (5), and x and y are the same as Eq. (6). Besides, from the relationship of x and y , Equation (7) is obtained. From Equations (5) and (7), the winding diameter of the second layer is derived as Eq. (8). Through Equations (4) and (8), a general mathematical model related to the increase of a winding diameter can be obtained as Eq. (9), and n in Eq. (9) indicates the number of stacked layers.

$$H_1 = D + d \tag{4}$$

$$H_2 = D + 2d + 2h \tag{5}$$

$$x = \frac{d}{2 \cos 30^\circ}, y = (x + d) \cos 30^\circ \tag{6}$$

$$h = y - d = \left(\frac{\sqrt{3} - 1}{2} \right) d \tag{7}$$

$$H_2 = D + 2d + 2h = D + (1 + \sqrt{3})d \tag{8}$$

$$H_n = D + (1 + (n - 1)\sqrt{3})d \tag{9}$$

By substituting Eqs. (1) and (2) for Eq. (9), the winding velocity according to the increase of a winding diameter is expressed as Eq. (10), and the traversing velocity is the same as Eq. (11) [4].

$$w_n = \frac{2U}{H_n} \tag{10}$$

$$V_n = \frac{Ud}{\pi H_n} \tag{11}$$

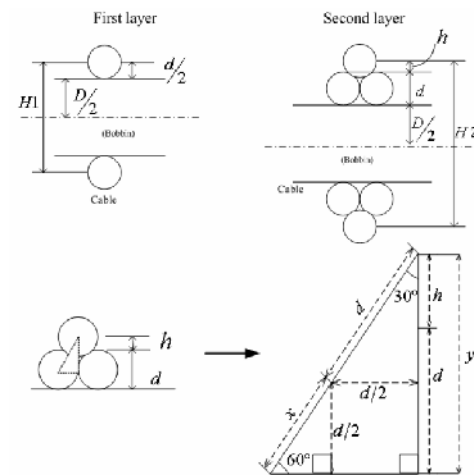


Fig. 2. Mathematical model of winding diameter.

2.2 A winding process model with bobbin shape error

From section 2.1, the mathematical modeling having no bobbin shape defect was carried out in an ideal case. However, the bobbin shape defect is one of the major reasons for pile up and collapse of a cable. These are critical problems in a high-speed cable winding system. Therefore, section 2.2 presents a winding model having the diameter error in the bobbin as Fig. 3 below.

In Eqs. (10) and (11), winding and traversing velocity are determined by the winding diameter in the bobbin. First, understanding the winding diameter in each position (CMD) should take precedence in the bobbin having the error (θ) in Fig. 3.

Fig. 4 shows that the first layer is being wound in the defective bobbin. N indicates the layer and m is the column wound. In Fig. 4, is the winding diameter of the first column in the first layer and is represented as Eq. (12).

$$H_{11} = D1 + 2(y1 + y2) = D1 + \frac{d}{\cos\theta} + d \tan\theta \quad (12)$$

From the geometrical relation as shown in Fig. 4, $y1$ and $y2$ are derived as Eq. (13).

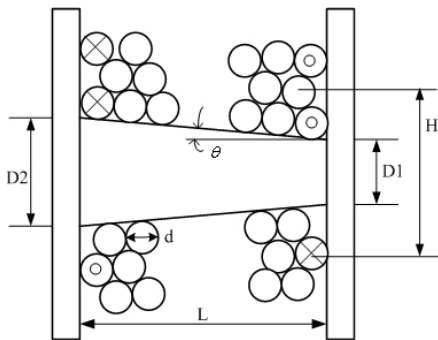


Fig. 3. A schematic of cable winding in defective bobbin.

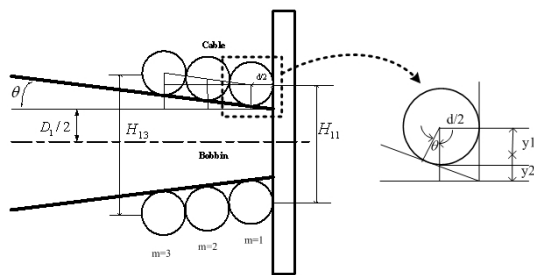


Fig. 4. The first layer in defective bobbin.

$$y1 = \frac{d}{2 \cos\theta}, y2 = \frac{d}{2} \tan\theta \quad (13)$$

Similarly, the winding diameter of the second column in the first layer is the same as Eq. (14).

$$H_{12} = D1 + \frac{d}{\cos\theta} + d \tan\theta + 2(d \sin\theta) \quad (14)$$

Eq. (15) indicates the generalized winding diameter in the first layer and that reflects the diameter error (θ) in the bobbin.

$$H_{1m} = D1 + \frac{d}{\cos\theta} + d \tan\theta + 2((m-1)d \sin\theta) \quad (15)$$

In Fig. 5, the second layer starts from the part that the first layer finished and the winding diameter of the first column in the second layer is represented as H_{21} . The distance between the centers of the last column in the first layer and first column in the second layer is represented as $y3$. It is derived as Eq. (16). The winding diameter value of the first column in the second layer is obtained by Eq. (17) in which H_{1a} is the winding diameter value of the last column in first layer.

$$y3 = d \sin(60 + \theta) \quad (16)$$

$$H_{21} = H_{1a} + 2 \times y3 \quad (17)$$

Through Eqs. (16) and (17), the winding diameter of the first column in the second layer can be obtained as Eq. (18). In this way, the winding diameter of the second column in the second layer is derived as Eq. (19).

$$H_{21} = H_{1a} + 2 \times y3 = H_{1a} + 2d \sin(60 + \theta) \quad (18)$$

$$H_{22} = H_{21} - 2(d \sin\theta) \quad (19)$$

The winding diameter generalized in the second layer is Eq. (20). Finally, the generalized mathematical model of the winding diameter in the bobbin having a winding diameter error is derived as Eq. (21).

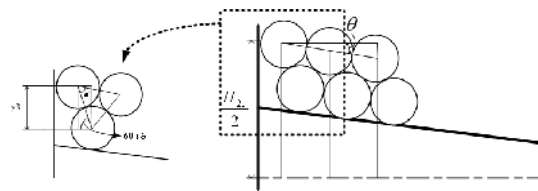


Fig. 5. The second layer in defective bobbin.

$$H_{2m} = H_{21} - 2((m - 1)d \sin \theta) \tag{20}$$

$$H_{nm} = D_1 + \frac{d}{\cos \theta} + d \tan \theta + ((-1)^n (a - 1) + (a + 1)) d \sin \theta + \sum_{s=1}^n (2d \sin(60 + (-1)^s \theta)) - 2d \sin(60 - \theta) + (-1)^{n-1} (2(m - 1)d \sin \theta) \tag{21}$$

By substituting Eqs. (10) and (11) for Eq. (21), Equation (22) is the winding velocity and Eq. (23) is the traversing velocity in the bobbin with the shape fault (θ). When the diameter error (θ) in the bobbin is zero, Eq. (23) and Eq. (24) are the same as Eq. (10) and Eq. (11), respectively.

$$w_{nm} = \frac{2U}{H_{nm}} \tag{22}$$

$$V_{nm} = \frac{Ud}{\pi H_{nm}} \tag{23}$$

2.3 Parameter analysis

When the winding operation proceeds in a bobbin having a diameter error, the winding diameter is increased and the winding and traversing velocity are changed. The conditions for the computer simulation are as in Table 1.

In Fig. 6, the increasing rate of the winding diameter is identical in each layer during the winding operation in the bobbin having a diameter error. However, the time that is taken to stack each layer is maintained constantly because the operating velocity is always constant. Thus the difference in the velocity change rate shown in Figs. 7-8 should be considered in the winding process adequately.

The velocity compensated is different in each layer and it is influenced largely in the early winding by the bobbin diameter error that is given as the initial condition of the system. In Fig. 7, dH1, the variation of the winding velocity, in the first layer is larger than dH5 in the fifth layer during winding. In this way, dL1 is larger than dL5 in Fig. 8.

The simulation results show that the bobbin shape fault greatly influences the initial winding. To overcome these shape errors, a velocity compensation of the winding and traversing based on the mathematical models (Eqs. (21-23)) is necessary.

The speed variation of the winding and traversing caused by the change of the operating velocity (40 and 18 m/min) are as follows. The simulation condi-

Table 1. Simulation conditions.

Variables	Values
Operating velocity [m/min]	40
Diameter of optical cable [mm]	7.2
Width of bobbin [mm]	200
Reference core diameter of bobbin [mm]	110
Core diameter fault of bobbin [θ , degree]	1.8

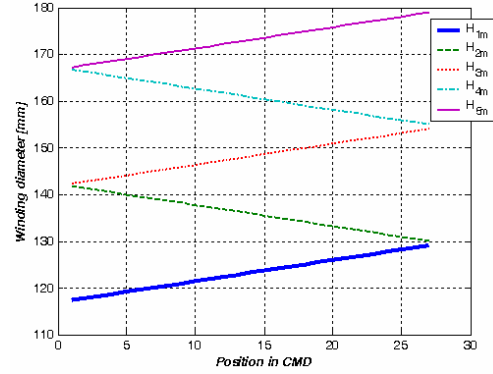


Fig. 6. Winding diameter variation in defective bobbin.

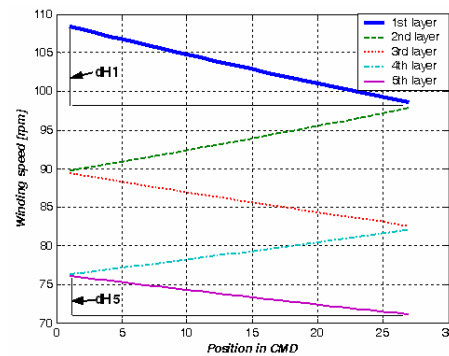


Fig. 7. Winding velocity variation in each layer.

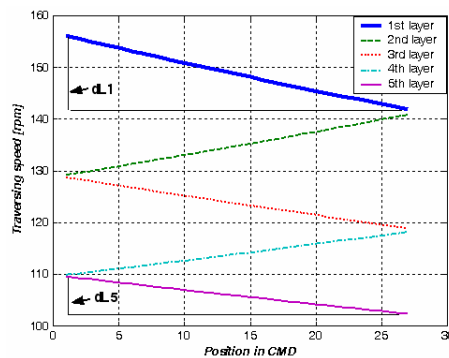


Fig. 8. Traversing velocity variation in each layer.

tions are such as in Table 2.

Figs. 9 and 10 show the velocity changes of the winding and traversing in each operating velocity. In Figs. 9 and 10, the winding and traversing speed variation of earlier winding process is larger than that of later winding process ($dWS1_{40\text{mpm}} > dWS1_{18\text{mpm}}$, $dTS1_{40\text{mpm}} > dTS1_{18\text{mpm}}$). In addition, the velocity variation of winding and traversing grows larger while the operating speed increases.

As a result, the variations of the winding and trav-

Table 2. Computer simulation parameters.

Variables	Values
Operating velocity [m/min]	40, 18
Diameter of optical cable [mm]	7.2
Width of bobbin [mm]	200
Reference core diameter of bobbin [mm]	110
Core diameter fault of bobbin [θ , degree]	1.8

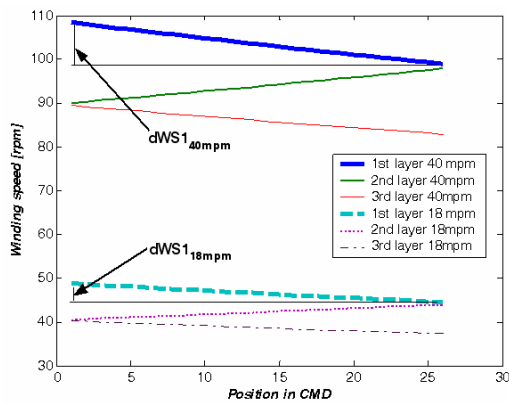


Fig. 9. Winding diameter variation in each layer (40, 18 mpm).

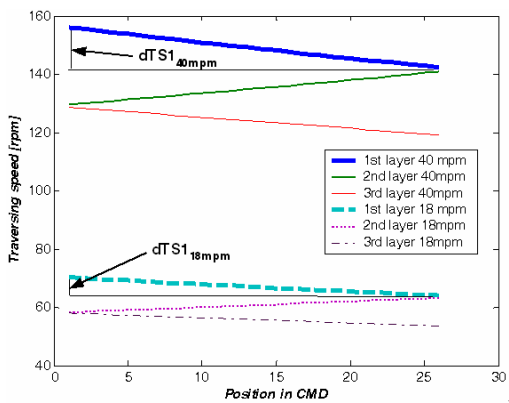


Fig. 10. Traversing velocity variation in each layer (40, 18 mpm).

ersing velocity are large in the bobbin with the diameter error when the winding process is in the first stage and the operating speed increases.

3. Visual feedback system

3.1 Machine vision system

Fig. 1 shows the visual feedback system to measure the diameter of the cable, the bobbin shape fault. The machine vision system for visual feedback consists of a CCD camera (JAI CV-S3200), image board (IMAQ PCI-1411) and image processing software (LabView). The image is converted into an analog signal by CCD camera, and this image signal is transformed into the

Table 3. CCD Camera (JAI CV – S3200).

Variables	values
Scanning system	NTSC:525 liens, 30 frame /sec
CCD sensor	Color 1/2 " IT sensor
Effective pixels	NTSC : 768 x 494
Cell size	NTSC : 8.4(h) x 9.8(v) μm
S/N ratio	>50dB

Table 4. Image board (IMAQ PCI-1411).

Variables	Values
Input signal	NTSC
Resolution	640 x 480, 320 x 240
Color format	RGB 24bit
Frame rate	30 frame/sec, 60 fields/sec
Image acquisition	Frame, Field

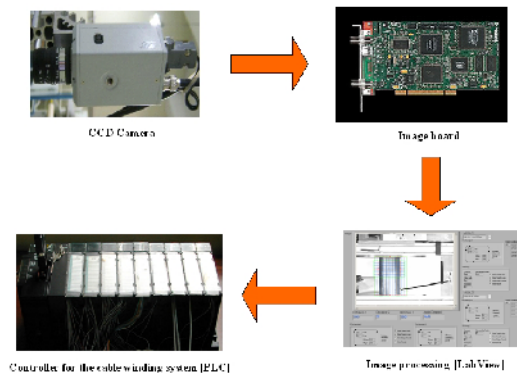


Fig. 11. Visual feedback systems.

digital format through the image board to be analyzed [5, 6]. The size of the digital image obtained is 640 pixels in width, 480 pixels in height and 1 pixel with 256 gray levels (8 bit). And then the image processing software carries out analysis of the image data. Finally, the result is transmitted to the main controller PLC (programmable logic controller).

Table 3 and Table 4 represent the major specifications of the CCD camera and the image board that are used.

3.2 Visual feedback

Fig. 12 represents fixing the range for the cable diameter measurement and shows the diameter value gauged. The measured diameter is about 7.23 mm, the real value is 7.3 mm. Using the measured value is suitable because the error is approximately 0.96%.

Fig. 13 shows the measured value of the bobbin shape fault. In is calculated by the measured D_1 , D_2 . Eq. (24), the bobbin shape error (θ)

$$\theta = \tan^{-1} \left(\frac{D_2 - D_1}{2L} \right) \quad (24)$$

4. Guiding system

4.1 A composition of the guiding system

Fig. 14 below shows the guiding system presented in this paper for high-speed self-align winding. The guiding system is an apparatus to minimize the pile-up and collapse of a cable and also to align the cable automatically at a high speed. The cable passes through between two idle rollers, and when it is placed at the edge of the bobbin, the system sticks the cables fast at both edges of the bobbin for its high-speed self-align and then returns it to the ongoing winding.

The LM guide (LMBM15, THK), an element consisting of the guiding system, minimizes the friction and load for the left-right movement of the guiding system. In addition, the ball screw (GY1520-0600A U type, KURODA) transforms the revolving motion of the AC servo motor (CN 08, FDA 5005, LGOTIS)—a driving motor of the guiding system, into a straight-line back-and-forth motion.

4.2 Operating principle of the guiding system

Fig. 15 shows an example of the pile-up and collapse of a cable occurring during the winding process. Through the observation and experiment on this phenomenon, it was confirmed that the pile-up and collapse of the cable occurred the most frequently at both edges of the bobbin. This is because there arises a case where the cable does not start at the edges of the bobbin when stacking up on new layers. Therefore, recognizing the instant the cable is placed at both edges of the bobbin by a non-contact amplifier photoelectric sensor (PZ-101, KEYENEC), the guiding system at the same time sticks the cable fast to the edge of the bobbin for the calculated time and then restores the cable to the original position after a given time lapses. In this case, we set the guiding system to fasten the cable after 0.8 revolution around the bobbin and then returned it to the original position, considering various factors such as the performance of the driving motor of the given guiding system, the lead distance (5mm) per round of installed ball screw, the working linear velocity 270 m/min, and the distance from the bobbin according to the installed location of the guiding system.

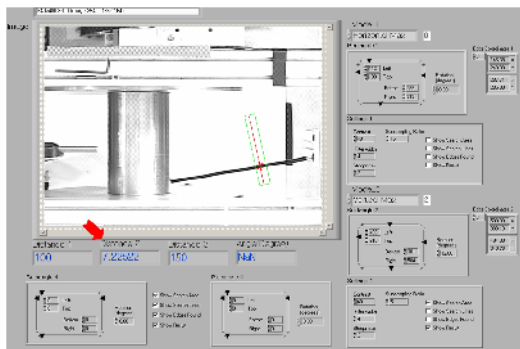


Fig. 12. Cable diameter measurement by using vision system.

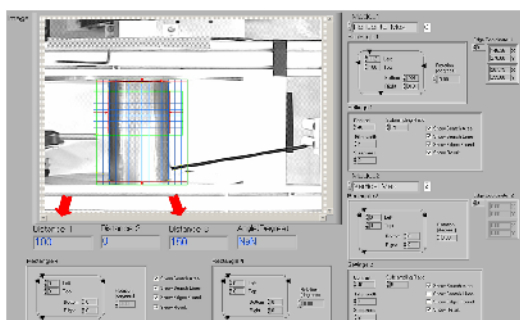


Fig. 13. Bobbin shape fault measurement by using vision system.

5. Real-time motion synchronization logic

5.1 Task definition of the winding system

A cable winding system is largely divided into three processes: winding, traversing and guiding. For these processes, we have defined the tasks as follows [8, 9].

5.1.1 Winding task

The winding task takes charge of the revolving motion of the bobbin and it requires keeping a constant tension when winding for the winding of an aligned cable.

The tension reacts sensitively to the velocity and thus the traversing velocity of the cable to the increase of winding diameter must be maintained at a constant value. Based on Eq. (22), a mathematical model of the winding velocity, the winding task operates from the initial process to the finishing one of the cable winding system, maintaining the traversing velocity of the cable at a constant speed when winding it.

5.1.2 Traversing task

It takes charge of the left-right linear motion of the bobbin. To prevent the pile-up and collapse of a cable, it is very important to synchronize the winding velocity with the traversing one. Based on the model expressed in Eq. (23), the traversing task operates from the start to finish of the process like the winding task, moving as much as the cable diameter per round of the bobbin.

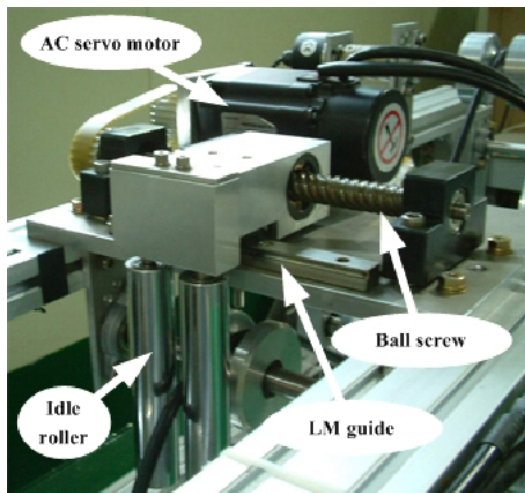


Fig. 14. Prototype guiding system.

5.1.3 Guiding task

As the task to the guiding system proposed in this study, it deals with the left-right straight-line motion of the guider. Errors like the pile-up and collapse of a cable mainly take place at both edges of the bobbin. For correction of these errors, the guiding task sticks the cable artificially fast to the edge of the bobbin when it is placed at the edge of the bobbin and then restores it to the original position.

5.1.4 Sensing and calculation task

By detecting through an infrared light sensor that the cable is placed at both edges of the bobbin, it begins the direction change of traversing, winding velocity change and the operation of the guiding system. Along with these, the calculation task is in charge of calculating the change of the traverse velocity change synchronized with the winding velocity, the change of the winding velocity to maintain a uniform tension, and the operating time of the guiding system for self-align winding.

5.1.5 User interface task

From the user interface module, user-entering functions such as the system start, stop and emergency stop are performed.

5.2 Real time controller for the self-align winding system

The self-align cable winding system presented in this study is largely composed of six tasks. The scheduling is carried out for improving the performance and guaranteeing stability of the system based on the exact motion synchronization. Fig. 16 shows a flow-chart for auto cable winding, each task operates in mutual correlation, and the operation time and operat-

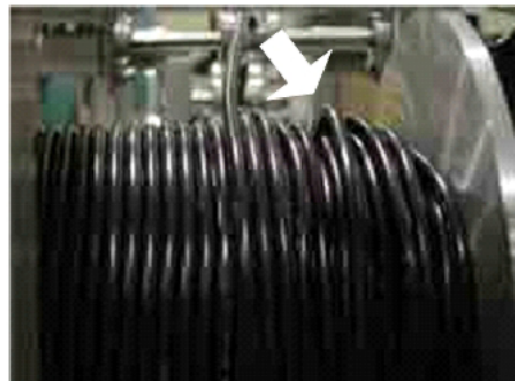


Fig. 15. Cable winding error.

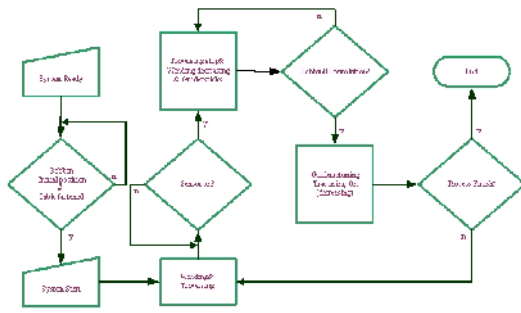


Fig. 16. Task flow table.

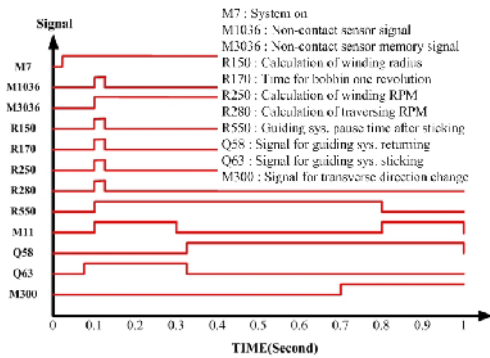


Fig. 17. Real-time scheduling for high speed self-align.

ing instant of each task are very important [10].

A reaction graph of each signal materialized in the PLC (programmable logic control) can be seen in Fig. 17, showing examples for signals being generated by real-time scheduling at the instant the cable is placed at both edges of the bobbin.

The most important thing for realizing the high-speed self-align cable winding is a mutual synchronization problem among three actuators (traversing, guiding, winding). This real-time scheduling is not just confined to the guiding system, but coupled with others like the winding and traversing.

6. Experimental results

Fig. 18 shows the schematic of the guiding system for the high-speed self-align winding. A simulator manufactured for the performance evaluation is shown in Fig. 19, consisting of an AC servo motor for winding, traversing and guiding, a non-contact sensor for sensing both edges, a load cell (OBBS-10, Bongshin) for measuring tension, an encoder to measure the traversing velocity of a cable, winding roll, unwinding roll, etc. In addition, an industrial controller

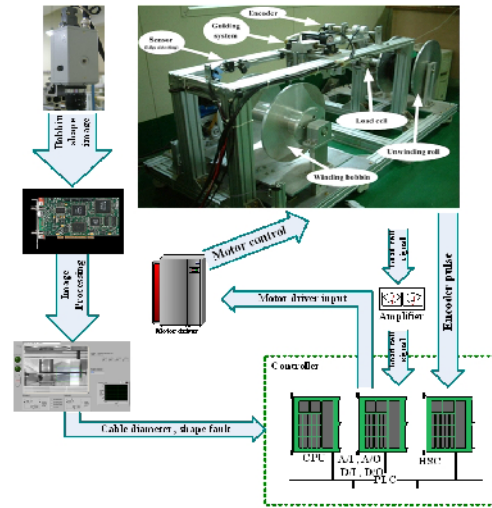


Fig. 18. Schematic of cable winding system.

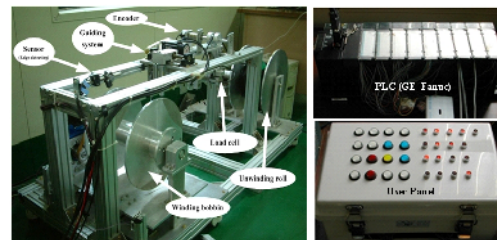


Fig. 19. Cable winding simulator with guiding system.

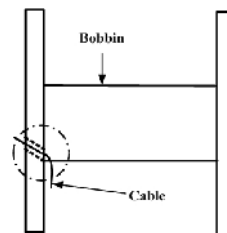
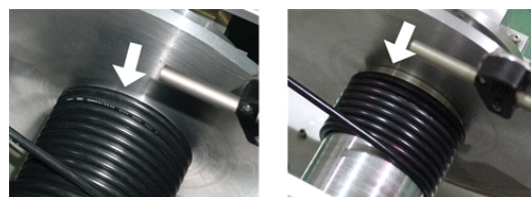


Fig. 20. Schematic of fastening the cable to the bobbin.



(a) With guiding system (b) Without guiding system

Fig. 21. Experimental results in the beginning of winding.

(GE-Fanuc PLC: LM90-30) was used considering working environments in the field and maximizing

Table 5. Experiment conditions.

Variables	Values
Cable diameter [mm]	7.2
Bobbin shape fault [Degree]	2
Bobbin width [mm]	200
Total winding layer	8

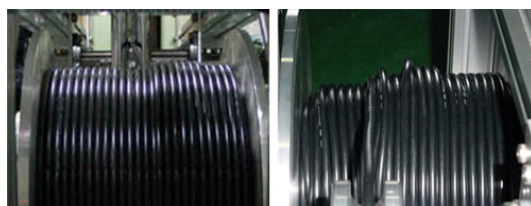
field applicability through the manufacture of the user panel.

Due to the cable rigidity, when starting the winding process, an error of having a gap at the combining part of the cable and bobbin often occurs and the gap becomes the cause of a cable collapse when stacking up the second layer. To prevent this, the initial error was minimized by fastening the cable to the bobbin as shown in Fig. 20.

Fig. 21 shows experimental results in the beginning of the winding process, showing a significant decrease of the gap occurring at the first layer by the self-align of the guiding system. The pile-up and collapse phenomena of the cable (Fig. 15) are much more influenced by the condition of the cable piled up on the previous layer rather than a defect of the currently piling layer. Fig. 21(a) shows a cable winding result with a guiding system, while the experimental result without a guiding system is shown in Fig. 21(b).

During the experiment, the linear velocity of the process was 300 mm/s, and the error usually occurs on the process start. In order to prevent this defect, the winding speed of the first revolution of the bobbin was set to 60 mm/s, one-fifth of the reference linear velocity. Nevertheless, as known from the result of Fig. 21, a relatively bigger gap at the end of the bobbin occurred in the case without guiding system mounted. A gap generated like this works as a major cause to produce the pile-up and collapse of the cable during stacking up the next layer.

Fig. 22 shows experimental results of a completed

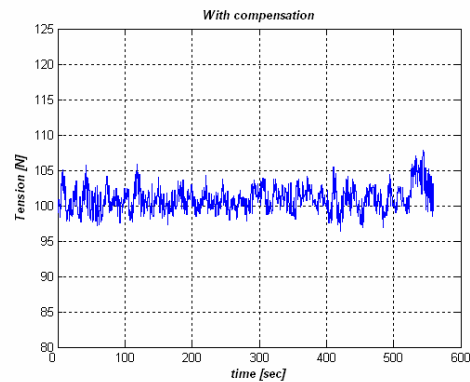


(a) With compensation (b) Without compensation

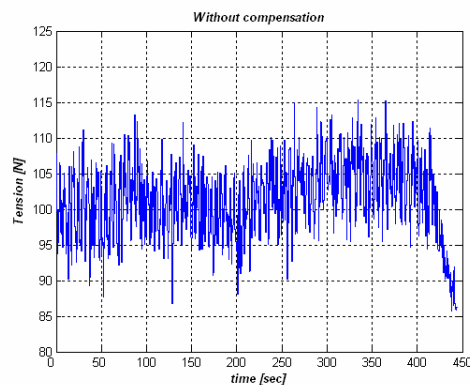
Fig. 22. Experimental results of high-speed cable winding.

cable winding process with a working linear velocity of 300 mm/s and Table 5 is experiment conditions.

Fig. 22(a) shows an experimental result of having completed shape fault compensation logic applied, while the experimental result with compensation logic removed is shown in Fig. 22(b). From the results of Fig. 22, it can be confirmed that the self-align of the cable can be effectively performed by the guiding system at the edges of the bobbin when winding at a high speed and by the bobbin shape fault compensation logic. Even in the case without bobbin shape fault compensation, it shows a relatively well-aligned winding condition up to about the third layer or so through the synchronization between each actuator and motion synchronization. The winding errors accumulate little by little and eventually cause the pile-up and collapse of the cable as in Fig. 22(b) because the cable is not wound until the end of the bobbin. Fig. 23(a) shows the tension variation of having shape fault compensation logic applied, while Fig. 23(b) shows the result with compensation logic removed. In



(a) With compensation



(b) Without compensation

Fig. 23. Tension variation in cable winding system.

Fig. 23(b), the value of tension is rising steadily and the magnitude of the tension disturbance is great. After all, the pile-up and collapse phenomenon of the cable is generated at 400 sec (Fig. 23(b)).

7. Conclusions

In this study and development, we have presented a mathematical model for the compensation shape fault. A guiding system for the high-speed self-align cable winding applied a real-time motion synchronization method and verified the performance of the guiding system experimentally by designing and manufacturing a simulator reduced to about 1/10 size of the actual one. Also, the modularization of the guiding system and a visual feedback system is applied in a high speed auto cable winding system.

As demonstrated through the experiment, it is expected that the application of the guiding system saves working manpower per facility and also improves productivity through the speed increase of product lines. The performance of the proposed shape fault compensation method is also validated.

In particular, a high-quality wound roll can be produced by using the proposed cable winding system.

Acknowledgment

This research was supported by the “Seoul R&BD Program (No.10848), Korea”.

References

- [1] K. H. Choi and S. C. Kim, Study of the Robotic Cell for the Filament Winding, Proceedings of the KSPE Autumn Annuals Meeting, Korea(1997) 1165-1168.
- [2] S. Y. Yang, Design and Experimental Verification on a Towing Winch, Journal of Control, Automation and System Engineering, 5 (1999) 489-496.
- [3] K. H. Shin, Tension Control, TAPPI Press, Technology Park/Atlanta (2000).
- [4] C. W. Lee, H. K. Kang and K. H. Shin, A Study on the Real-time Synchronization of Motions in a Self-align Cable Winding System, Proceedings of the KAMES Joint Symposium A, Korea (2002) 845-849.
- [5] I. C. Peter, Visual Control of Robots, Research Studies Press LTD (1996).
- [6] K. Thomas, Image Processing with LabVIEW and IMAQ Vision, Prentice Hall (2003) Chap. 1-4.
- [7] S. Milan, H. Vaclav and B. Roger, Image Processing, Analysis and Machine Vision ITP (1999), Chap. 1-3.
- [8] C. W. Lee, H. K. Kang, and K. H. Shin, Development of a Guiding System for the High-speed Self-align Cable Winding, Journal of the Korean Society of Precision Engineering, 21 (2004), pp.124-129.
- [9] J. Liu, Real-time Systems, Prentice Hall (2000) 115-179.
- [10] B. K. Kim, Control Latency for Task Assignment and Scheduling of Multiprocessor Real-time Control Systems, International Journal of Systems Science, 30 (1999) 123-130.



Chang-woo Lee received a B.S. degree in Mechanical Engineering from Konkuk University in 2001. He received his M.S. and Ph.D. degrees from Konkuk university in 2003 and 2008, respectively. Dr. Lee is currently a researcher at the Flexible Display Roll to Roll Research Center at Konkuk University in Seoul, Korea.

Dr. Lee's research interests are in the area of fault tolerant control, R2R e-Printing line design, and tension-register control. He is the holder of several patents related to R2R e-Printing system.



Hyankyoo Kang received the B.S. and M.S degree in 2000 and 2003 respectively from Konkuk University, Seoul, Korea, where he is currently working toward the Ph.D. degree in mechanical design. He took part in the development of an autoalign guiding system for high-

speed winding in a cable winding system, a 3-D roll-shape diagnosis method in a steel rolling system, a design of register controller for high-speed converting machine and real-time control design of electronic printing machine. His research topics include register modeling and control for printed electronics and distributed real-time control.



Kee-Hyun Shin (S'81–M'02) received the B.S. degree from Seoul National University, Seoul, Korea, and the M.S. and Ph.D. degrees in mechanical engineering from Oklahoma State University (OSU), Still-water. Since 1992, he has been a Professor with the Department of Mechanical and Aerospace Engineering, Konkuk University, Seoul, Korea. For more than 18 years, he has covered several research topics in the area of web handling, including tension

control, lateral dynamics, diagnosis of defect rolls/rollers, and fault-tolerant real-time control in the Flexible Display Roll-to-Roll Research Center, Konkuk University, of which he has also been a Director. His research topics include distributed real-time control, embedded control, monitoring, and diagnosis and fault-tolerant control of large-scale systems such as steel plants, film-and-paper-making plants, aircraft, ships, and ubiquitous control of multirobot systems. He is the author of *Tension Control* (TAPPI Press, 2000) and is the holder of several patents related to R2R e-Printing system.